

Chapter 5

Development of Carbon Nanotube Reinforced Aluminum Matrix Composite Brake Drum for Automotive Applications

Meenakshi Sundaram. U^{*1}, Mahamani. A²

^{*1}Department of Mechanical Engineering, Dilla University, P.O Box 419, Geddo Zone, Dilla, Ethiopia

²Department of Mechanical Engineering, Sri Venkateswara College of Engineering and Technology, Chittoor -517127, A.P, India

^{*1}ums.kiruthiga@gmail.com; ²mahamanisudhan@gmail.com

I. INTRODUCTION

The present chapter discusses the integration of carbon nanotube reinforced aluminum matrix composites for the application of the automotive brake drum. Generally, aluminum matrix composite is a technique enabling to tailor the desired properties to suit the appropriate application. Automotive and aircraft industries are aspiring for weight reduction to promote the mileage of the vehicle. The advantage of the aluminum matrix composites are: lower density, higher specific mechanical properties, better thermal conductivity and lower coefficient of thermal expansion than the unreinforced alloy. These attractive properties are stimulating the material designer to replace existing material with composites. However, the obstacles for the conversion of composites into engineering components are: high cost reinforcement, poor dispersion, agglomeration, and excessive tooling cost. Existence of higher volume and macro size wear resistant particles limits the properties and manufacturability of the engineering components. Higher volume fraction in the composites reduces the ductility, which restricts formability of the material. Whereas, the presence of the macro size reinforcements confines the dispersion of the particle in to the matrix. Hence, the interfacial bonding between the particle and matrix gets diluted which reduces the mechanical properties of materials.

The above discussion suggests for developing materials with lesser volume fraction and smaller reinforcement particles. Dispersion of the nano size reinforcement particles with lesser volume fraction is the right choice to enhance the composite properties without compromising the associated density. For the proposed composites, A 356 alloy is used as a matrix material. A 356 alloy is groups of hypo eutectic Al-Si alloy which possess good mechanical properties at room temperature as well as at elevated temperature. This alloy is widely used in the automotive and avionics industries. Hence, A356 alloy is selected as matrix material for the current investigation. Grey cast iron is the existing material for brake drum, which possesses more weight. The present investigation aims to find a replacement for the existing brake drum material by A356 carbon nanotube composite. The brake drum used in automobile is subjected to severe wear from the brake shoes. Therefore, the current study requires dry sliding wear experimentation, where pin on disc experimental setup is preferred for the investigation. The pin material is prepared by using the commercial car lining materials. Disc is prepared by carbon nanotube reinforced A356 aluminum matrix composites and grey cast iron for wear test. The literature survey exposes that, wear studies on the carbon nanotube reinforced A356 aluminum matrix composites for the application of brake drum was not addressed by other authors. Therefore, the present investigation deals with the wear behavior of the carbon nanotube reinforced composites. The present investigation is aimed to synthesize the nanoaluminum dross-fly ash-carbon nanotube A356 aluminum matrix composites with different reinforcement ratio and characterize the composites with EDAX (Energy Dispersive Analysis of X-rays), XRD (X-Ray Diffraction) and SEM (Scanning Electron Microscope) techniques, evaluate wear behavior of the composites, and compare the mechanical and wear behavior of the composites with the existing brake drum materials. In addition, the influence of sliding velocity and normal load on wear performance is studied. Also, wear rate, wear resistance and coefficient of friction are investigated under different reinforcement ratio, sliding velocity and normal load. It is expected that the addition of carbon nanotubes into the matrix will enhance the wear performance. By establishing the wear behavior of the proposed composites, it is possible to draw a conclusion for the replacement of the existing brake drum materials by the composites. Relatively lower density components promote the weight reduction, which will reduce the fuel consumption.

This chapter consists of seven sections. Section one is an introductory part, section two discusses about literature survey, section three materials and methods used for the study, section four discusses about experimental work executed to carry

out the work. Analysis of results with respect to wear data and coefficient friction are discussed in section five. Analysis of worn out surface with SEM images are discussed in section four. Section seven gives the conclusions on the research findings.

II. LITERATURE SURVEY

There are many techniques for the production of metal matrix composites with CNT as reinforcement and it has been addressed by many authors. Shadakshari et al. [1] have studied different mixing techniques like high energy ball milling, low energy ball milling, polyester binder-assisted (PBA) mixing for Al-CNTs powder preparation to prove that CNTs are a promising reinforcement for metal matrix composites. Threrujirapong et al. [2] have studied friction and wear behavior of CNT reinforced titanium matrix composite under dry sliding conditions and concluded that friction coefficient of specimens were decreased with increasing MWCNT content and applied load. Al-Aqeeli [3] has studied processing of Al-based CNT reinforced composites using different consolidation techniques and observed that mechanical alloying technique is a successful method in finely dispersing the CNT's into the Al-based alloy matrix. Liu et al. [4] studied singly dispersed carbon nanotube/aluminum composites fabricated by powder metallurgy combined with friction stir processing (FSP) and concluded that FSP could break down the CNT clusters and disperse the carbon nanotubes into the matrix, and the distribution homogenization of the CNTs increased with increasing FSP pass. Jinzhi et al. [5] have undertaken studies on carbon nanotube evolution in aluminum matrix during composite fabrication process and found that CNTs were damaged during mechanical powder mixing and sintering process. Sehyun et al. [6] have studied the manufacture of CNTs-Al powder precursors for casting of CNTs-Al matrix composites and found that a uniform distribution of CNTs strongly depends on the milling time. As milling time increases, CNTs were fractured by ball-to-ball collisions.

Kim et al. [7] found that Cu coated on the surface of MWCNTs plays an important role in uniform distribution reinforcement within Al matrix, enhancing good interfacial strength between two interfaces and efficient stress load transfer through MWCNTs in Al matrix. Kwon and Leparoux [8] have studied the Al-CNT composite powders obtained by a powder metallurgy route and showed fine mean particle size distributions with an increasing amount of CNT addition. The hardness also increased with an increase in the CNT content. Unnikrishnan et al. [9] have undertaken studies on the processing and characterization of aluminium-silver coated MWCNT composite made by vacuum hot pressing; their results show that composite mixed with 1 wt% of silver coated CNT gives relative density and hardness almost equal to composite made with 4 wt% of uncoated CNT. Kwon et al. [10] have fabricated functionally graded CNT-reinforced MMC bulk materials by a hot-pressing method and they reported that hardness of the 15 vol% CNT composite was more than the unreinforced Al. Alba-Baena et al. [11] have made a study on Al-MWCNT aggregate, where two phase composites of 2 and 5% volume fraction were fabricated using a single tube shockwave consolidation process. Vickers hardness was dramatically increased with increasing of the amount of CNT addition. Lima et al. [12] have used friction stir processing to produce an aluminum alloy reinforced with multi-walled carbon nanotubes. It was found that when tool rotation speed is increased from 1500 and 2500rpm and increasing the tool shoulder penetration depth improved the distribution of CNTs in the Al-alloy matrix. Abbasipour et al. [13] have produced A356 aluminum alloys reinforced with carbon nanotubes (CNTs) which were produced by stir casting and compocasting routes and they were examined for microstructural characteristics and hardness. Injection of Ni-P-CNT coated aluminum particles alleviates the difficulties of poor wettability, agglomeration and gravity segregation of CNTs in the melt. Laha et al. [14] developed an Al-based nanostructured composite with carbon nanotubes as second phase particles and has been synthesized by plasma spray forming technique. They found that the composite experienced an increase in relative microhardness due to the presence of carbon nanotube. Noguchi et al. [15] introduced totally new principle, and succeeded in producing nano-scale composites in which CNTs were uniformly dispersed in Al matrices. They named this method Nano-Scale Dispersion (NSD) method. The composites obtained were found to be highly reinforced and not to melt at a temperature far above the melting point of Al. Senthil et al. [16] used high energy ball mill to disperse multi-walled carbon nanotubes in AA 4032 alloy. MWNTs and were dispersed homogeneously in the AA4032 matrix composites. Effects of milling time on grain size and lattice strain were studied and there was decrease in grain size and increase in strain with increase in milling time.

Morisada et al. [17] were successfully achieved to disperse multi-walled carbon nanotubes (MWCNTs) into a magnesium alloy (AZ31) using friction stir processing (FSP). The FSP with MWCNTs obviously increases the microhardness of the composites. The maximum microhardness of these composites was 78 Hv, which is almost double that of the AZ31 substrate (41 Hv). Lu et al. [18] have improved the wear resistance of magnesium alloys, nano-alumina (n-Al₂O₃) particles and CNTs reinforced AZ31 magnesium alloy matrix composites and hybrid composites which were fabricated by friction stir processing (FSP). All the composites were more resistant in wear than FSP AZ31 alloy. Lin et al. [19] have undertaken dry wear tests to investigate the tribology properties varying with the contents of CNTs, the sliding velocity and the normal loadings on martensitic S45C carbon steels and the copper matrix composites with 5, 10, 15 and 20 vol.% CNTs, which were fabricated by the vacuum sintering method. The friction coefficient increases as the content of CNTs decreases and the wear rate shows the lowest value when the carbon nanotubes content is 10–15 vol.%. Habibiet al. [20] have undertaken analysis on Mg/Al–CNT nano-composites which were fabricated using powder metallurgy route involving microwave assisted rapid sintering and hot extrusion. Ball milled Al–CNT particles comprising different contents of CNTs coated with fixed amount of Al were used for strengthening. They showed that nano-composite configurations

exhibit different tensile and compressive response as a function of CNT content. Among the different Mg/Al–CNT formulations synthesized, the Mg/Al–CNT configuration with Al–CNT particles composition of 1.00% Al and 0.30% CNT by weight (Mg/1.00Al–0.30CNT) exhibit higher tensile yield strength (YS) (0.2%), ultimate tensile strength (UTS) and failure strain (FS) (up to +72%, +48%, +9%, respectively) compared to monolithic Mg. Carvalho et al. [21] produced an AlSi–CNTs functionally graded material (FGM) that can be considered for engine compression piston rings. The AlSi graded composites (reinforced with 0–2 wt.% CNT FGM approach) was obtained with a new equipment that was designed to produce FGMs by powder metallurgy (PM) processing route. The best mechanical properties for homogeneous specimens were obtained in the case of 2 wt.% CNTs, while the best wear results were obtained in the case of 6 wt.% CNTs. Thus, the 2 wt.% of CNTs composite was chosen to produce the FGM since it was the composition that has the best compromise between mechanical and wear properties. Koji Kato and Koshi Adachi [22] have characterized the modes of wear of ceramics as mild wear and severe wear. For mild wear, tribochemical reaction forms a relatively soft and thin surface layer which is detached from the surface as thin flakes. In case of severe wear, the wear debris is formed by mechanical cracking of grains or delamination of tribo-films on the scale of the grain size. Nuno Silvestre et al. [23] presented a molecular dynamics (MD) study on the characterization of the compressive behavior of an aluminum (Al) material reinforced with carbon nanotubes (CNTs). They showed that in comparison with pure Al, the Young's modulus increases about 50% in case A (displacements imposed only to Al atoms at the boundary) and 100% in case B (displacements imposed to both Al and C atoms at the boundary). These increases are not only due to the CNT intrinsic stiffness but also to the interface slip stresses, which are about 16 MPa (case A) and 75 MPa (case B). In opposition, it is seen that both yield stress and yield strain do not increase. This evidence is mostly due to premature failure of the CNT–Al composite due to CNT local buckling.

Peng and Chang [24] have applied mechanical alloying (MA) to disperse CNT in the aluminum matrix. Both stearic acid and ethanol were used as process control agents (PCA) to control the properties of particles. Research results indicate that mechanical alloying is an effective way to achieve homogenous distribution of CNT in the Al matrix. Ethanol as process control agent promotes the refinement of Al particles but also increases the damage of CNT during the ball milling process. In the research investigation undertaken by Esawi et al. [25], have used ball milling to disperse MWCNTs of two different morphologies (stiff and straight vs. bent and entangled) as well as two different sizes (very large diameter and 3.5 times smaller diameter) in aluminium powders, which were subsequently hot consolidated by hot extrusion. The effect of milling time (up to 48 hours) on the morphological development of the powders and dispersion of CNTs was investigated. The results show that the technique is effective in dispersing the nanotubes within the soft Al matrix which simultaneously protects the nanotubes from damage under the impact of the milling balls. Liao and Tan [26] studied the mechanical mixing methods, viz. high energy and low energy ball millings, and compared them to a novel polyester binder-assisted (PBA) mixing method. Experimental results showed that the high energy and low energy ball-milled CNTs disintegrated and there were residual stresses, unlike the PBA-CNTs. Alfonso et al. [27] have analysed the effect on Young's modulus of Al_4C_3 formation in the carbon nanotube (CNT)–Al interface by using Finite Elements Analysis. The incorporation of the different CNT volume fractions and interfacial Al_4C_3 layers of various thicknesses are investigated. It is observed from the analysis the elastic modulus of the composites significantly increased by increasing the CNT volume fraction.

Biao Chen et al. [28] have developed a solution ball milling (SBM) approach to homogeneously disperse CNTs in Al matrix composites (AMCs). The tensile strength of Al matrix was noticeably enhanced by CNT additions agreeing with the potential strengthening effect predicted by the load transfer mechanism. Zhou et al. [29] indicated that the friction coefficient of the composite decreased with increasing the volume fraction of CNTs due to the self-lubrication and unique topological structure of CNTs. Within the range of CNTs volume fraction from 0% to 20%, the wear rate of the composite decreased steadily with the increase of CNTs content in the composite. Xudong et al. [30] studied the even deposition of Ni catalyst onto the surface of Al powder by impregnation route with a low Ni content (0.5 wt.%) and in situ synthesis of carbon nanotubes in Al powder by chemical vapor deposition (CVD). The in situ synthesized CNTs with well-crystallized bamboo-like structure in the composite powders can obviate the reaction with Al below 1000 °C. The feasibility of fabricating CNT/Al composites with high mechanical properties using the as-prepared composite powders was proved by their primary test, which indicated that the compressive yield stress and youngs modulus of 1.5 wt.% CNT/Al composites synthesized by hot extrusion are 2.2 and 3.0 times as large as that of the pure Al matrix. Esawi and Morsi [31] used mechanical alloying (MA) for the first time to generate a homogenous distribution of 2 wt% CNT within Al powders. The effect of milling time (up to 48 hours) on the morphological development of the powders and dispersion of carbon nanotubes was investigated. The results show that the technique is effective in dispersing the nanotubes within the soft aluminum matrix which protects the nanotubes from damage under the impact of the milling balls. Choi et al. [32] have worked on strengthening behavior of the ultrafine-grained A2024 and the A2024/MWCNT composite, fabricated using a hot rolling process involving ball-milling techniques. The A2024 matrix composite containing 3vol.% MWCNTs exhibits a yield stress of 780 MPa in tension. Age hardening increases the hardness further. The composite shows the peak hardness after 4 hours of aging because MWCNTs also act as a pathway for diffusion of atoms. Niranjana and Lakshminarayanan [33] have studied the wear behaviour of Aluminium matrix/titanium diboride reinforced (Al/TiB₂) composites by using a pin-on-disc wear tester at room temperature. It is found that the wear properties of MMC has improved significantly than the unreinforced alloy.

From the literature survey it is evident that wear studies on the carbon nanotube reinforced A356 aluminum matrix composites for the application of brake drum was not addressed by other authors. So an attempt is made to develop A356 MWCNT Composite for brake drum for automotive applications.

III. MATERIALS AND METHODS

In the present work A356 aluminum alloy is used as the matrix and multi walled carbon nanotubes are used as reinforcement. Abbasipour et al. [13] have produced A356-CNT composites by a special reinforcement technique and compocasting route and found that hardness of the samples are increased significantly with the addition of CNTs. To validate the fabricated material for break drum application, wear test is to be conducted and the wear performance of A356-MWCNT composites are to be compared with wear performance of conventional break drum material such as Gray cast iron.

MWCNTs with 98% purity and outer diameter Av 20 nm were acquired from United Nanotech Innovations PVT Ltd., Bangalore, India. The Technical Data of MWCNT is shown in Table 1. A scanning electron microscopy (SEM) image, Transmission electron microscopy (TEM) image and Raman spectra of the as-received MWCNTs are shown in Figs. 1-3, respectively.

TABLE 1 MULTIWALL CARBON NANOTUBE DATA SHEET

MWCNT	Description	Characterization method
Production method	Chemical Vapor Deposition (CVD)	Proprietary Method
Available form	Black powder	visual
Diameter	Av. Outer Diameter: 20nm	TEM, SEM
Length	Av 20 μm	SEM, TEM
Nanotubes purity	>98%	TGA,RAMAN
Metal particles	<1%	TGA
Amorphous carbon	<1%	TGA,XRD
Specific Surface area	330 m^2/g	BET
Bulk density	0.20-0.35 g/cm^3	Pycnometer

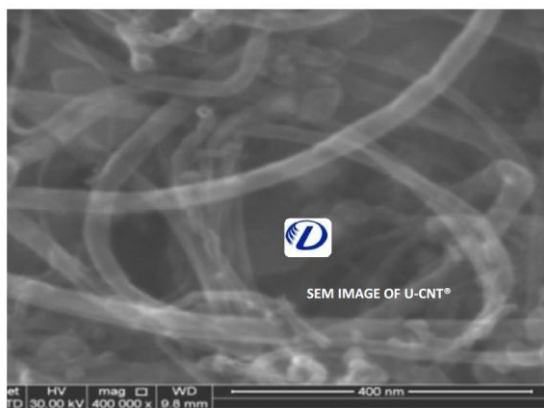


Fig. 1 SEM image of MWCNT

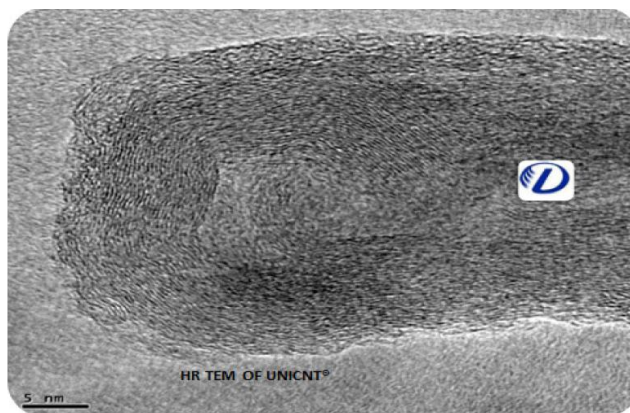


Fig. 2 TEM image of MWCNT

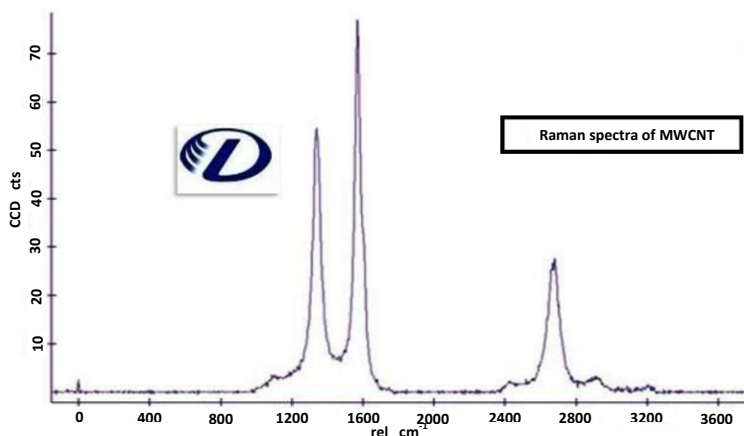


Fig. 3 Raman spectra of MWCNT

A356 Aluminum alloy generally find its applications in aircraft pump parts, automotive transmission cases, aircraft fittings and control parts and water-cooled cylinder blocks. It is having excellent castability, good weldability, pressure tightness, and good resistance to corrosion. A356 was procured from RSA Metal, Coimbatore, India. Its composition is given in Table 2 and SEM image, EDAX analysis, XRD analyses are given in Figs. 4-6, respectively.

TABLE 2 CHEMICAL COMPOSITION OF A356 ALUMINUM ALLOY

Constituent	Percentage
Al	90-93
Si	6-7.5
Mg	0.45
Cu	0.25
Mn	0.35
Fe	0.6
Ti	0.25
Zn	0.35

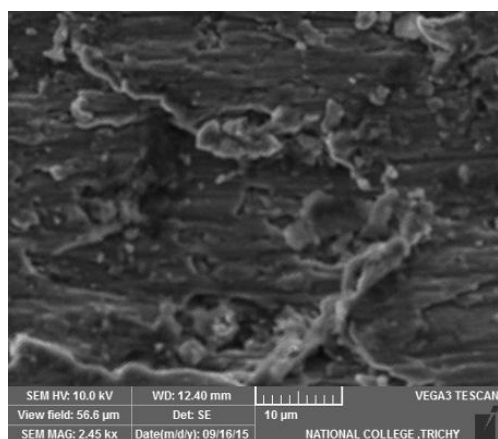


Fig. 4 SEM image of pure A356 aluminum alloy

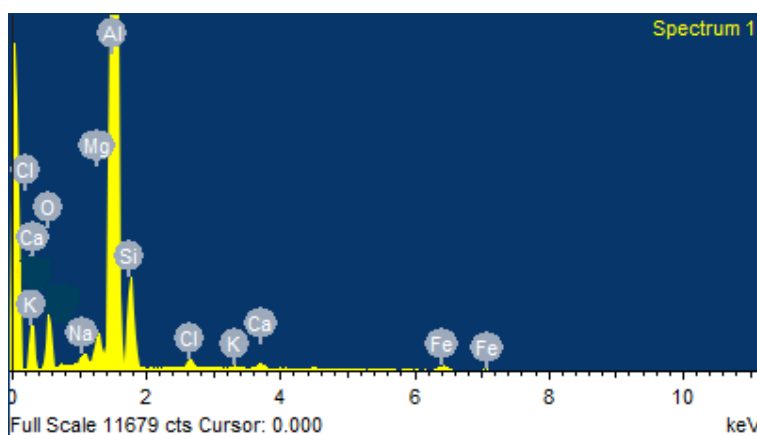


Fig. 5 EDAX Analysis of pure A356 aluminum alloy

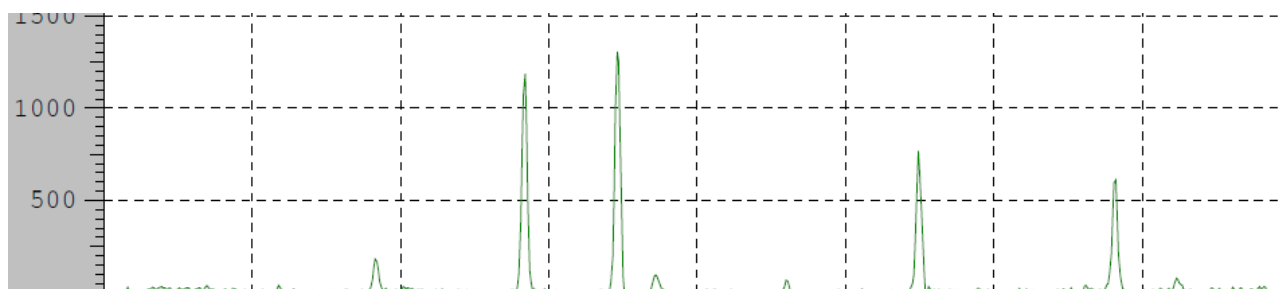


Fig. 6 XRD spectrum of pure A356 aluminum alloy

Chemical composition of gray cast iron is given in Table 3. Its SEM image and XRD analysis are given in Figs. 7-8, respectively.

TABLE 3 CHEMICAL COMPOSITION OF GRAY CAST IRON

Constituent	Percentage
Fe	93
C	3.2-3.5
Mn	0.6-0.9
P	0.12
S	0.15
Si	2.2

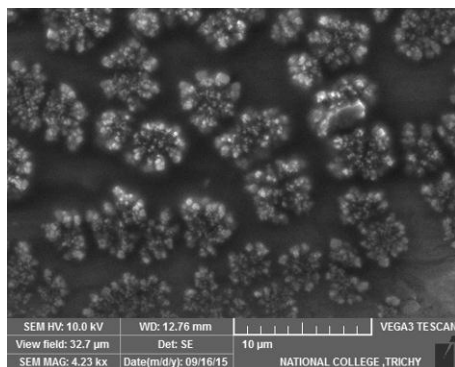


Fig. 7 SEM image of gray cast iron

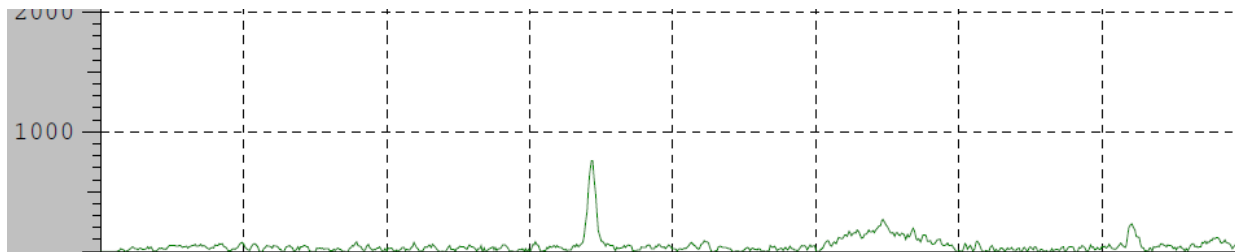


Fig. 8 XRD spectrum of gray cast iron

A356-MWCNT composites were produced by a special compocasting method [13]. Fig. 9 schematically shows the experimental set-up used in the production of composites. A ceramic crucible is placed in a muffle furnace. A coated injection tube is inserted in to the crucible to introduce the reinforcement. A coated steel stirrer is present at the centre to mix the liquid A356 with MWCNT. The reinforcement was injection of into the melt using Argon gas. Small size particles have high tendency for agglomeration and it is a great obstacle for uniform dispersion of MWCNT in the melt. In order to improve the wettability of carbon nanotubes with the melt and to reduce their agglomeration and to obtain a good distribution of carbon nanotubes in the matrix carbon nanotubes were injected into the melt in the form of carbon nanotubes deposited aluminum particles instead of raw carbon nanotube powder.

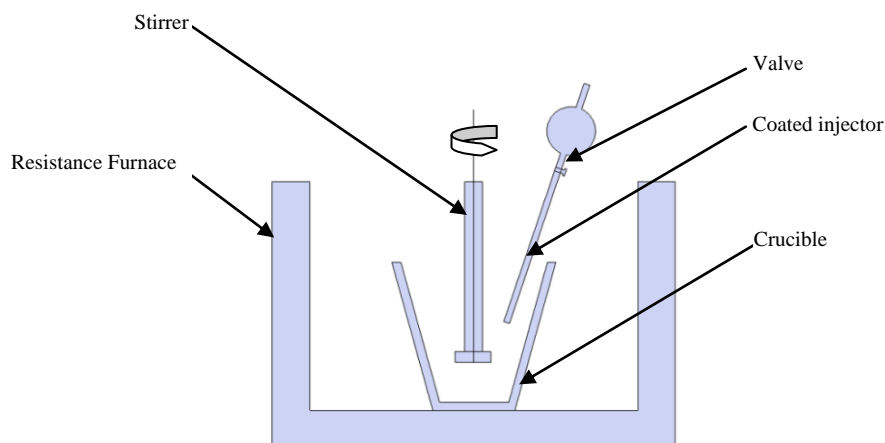


Fig. 9 Schematic arrangement stir casting furnace

To prepare CNT deposited aluminum particles Ni-P electroless plating technique was used. First purification and pretreatment of CNTs and aluminum particles were done by degreasing, acid-treatment and ultrasonic cleaning. Then coating of aluminum particles with Ni-P-CNTs was performed. A commercial electroless solution was used as electroless acid plating bath. Sodium hypophosphite is used as reducing agent and nickel sulphate is used as nickel source. Mass ratio of 6:1 between aluminium powder to CNT was chosen for the electroless plating bath. The CNT deposited aluminum particles were injected into the melt at a temperature of 700 °C which is well above the liquidus temperature of A356. During injection process the melt is being stirred uniformly to increase the wettability between the matrix and the reinforcements 1% magnesium (mass fraction) was added to the melt. After completion of the injection, the slurry was cast into a cylindrical steel mould as shown in Fig. 10.



Fig. 10 Composites are casted in a cylindrical steel die, (a) before casting, (b) after casting

Samples with four different volume fractions (2%, 4%, 6%, and 8%) are processed and poured into a preheated cylindrical metallic mould. Then the solidified casting was removed and subjected to T6 heat treatment. To make a comparative study one disc of pure A356 aluminum alloy was also prepared. To prepare test specimens for micro hardness, SEM, EDAX analysis and characterization a small billet of size 10mm thick and 100 wide with available height is also casted in a square steel die along with the above preparation. Fig. 11 shows the cast composite discs and billets. Fig. 12 to 23 shows SEM image, EDAX analysis and XRD analysis of MMC for various volume fractions respectively.



Fig. 11 Cast composite discs and billets

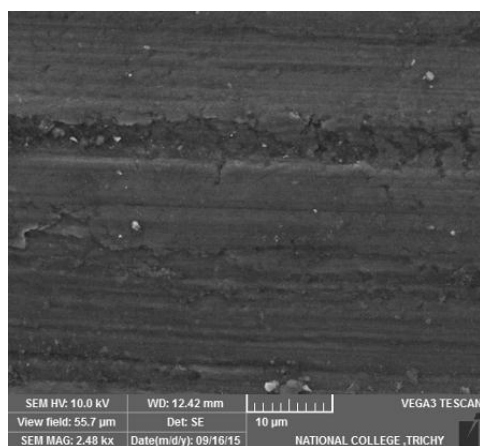


Fig. 12 SEM image of A356-2% vol MWCNT

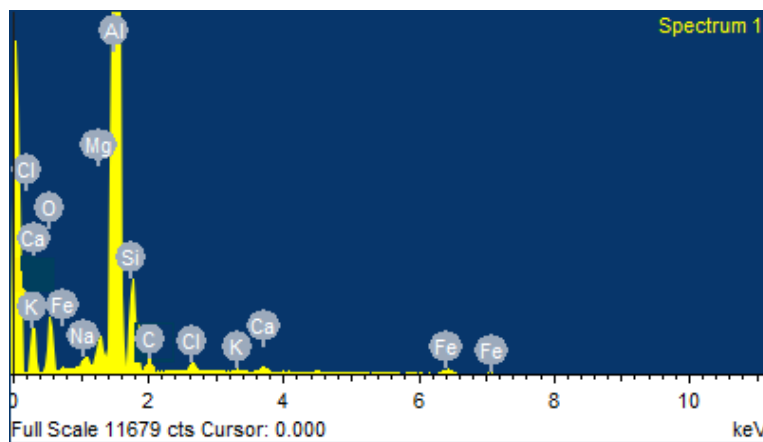


Fig. 13 EDAX image of A356-2% vol MWCNT

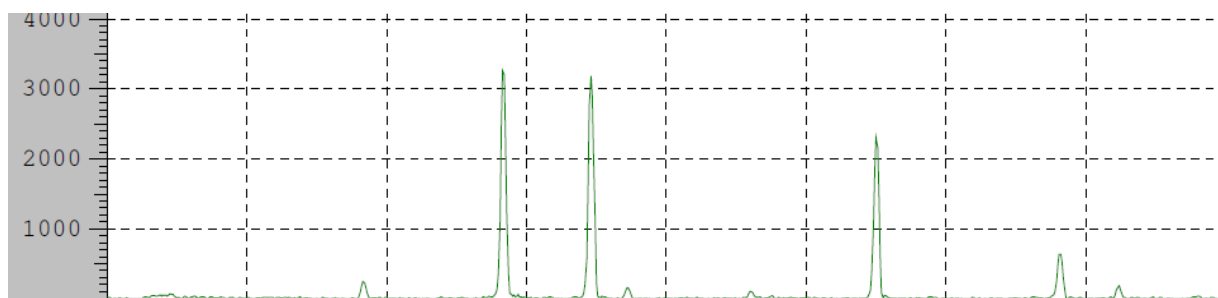


Fig. 14 XRD spectrum of A356 composite reinforced with 2% vol MWCNT

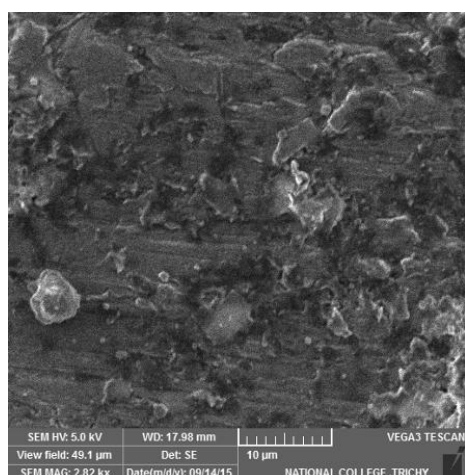


Fig. 15 SEM image of A356 -4% vol MWCNT

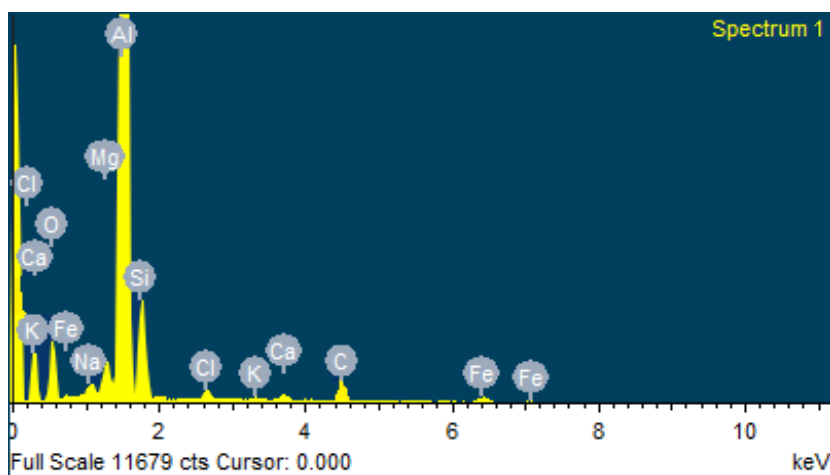


Fig. 16 EDAX image of A356-4% vol MWCNT Composite



Fig. 17 XRD spectrum of A356 composite reinforced with 4% vol MWCNT

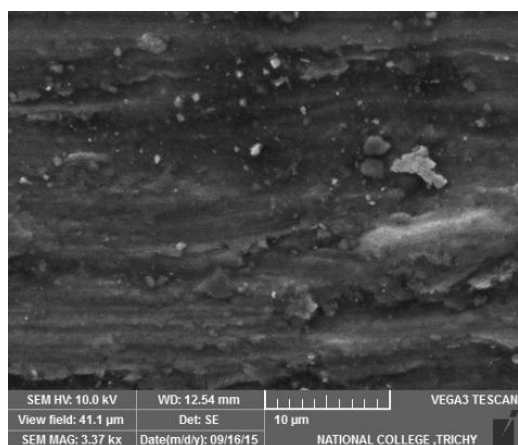


Fig. 18 SEM image of A356-6% vol MWCNT composite

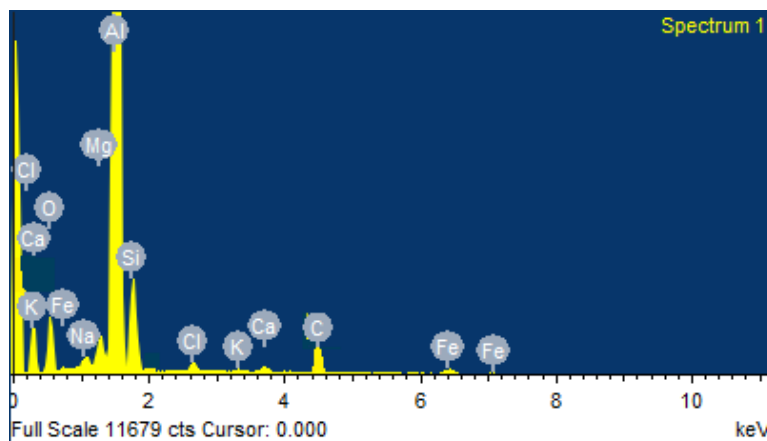


Fig. 19 EDAX image of A356-6% vol MWCNT composite

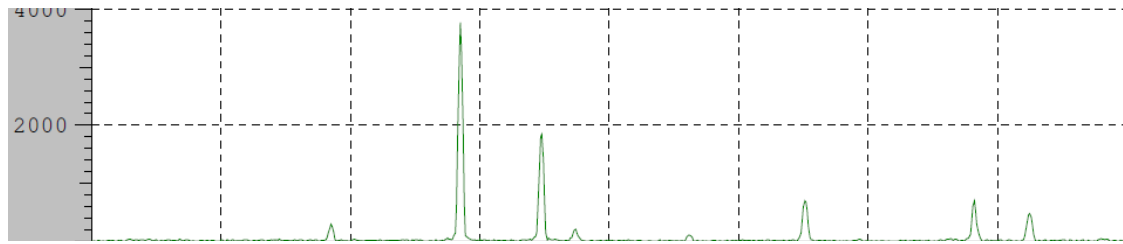


Fig. 20 XRD spectrum of A356 composite reinforced with 6% vol MWCNT

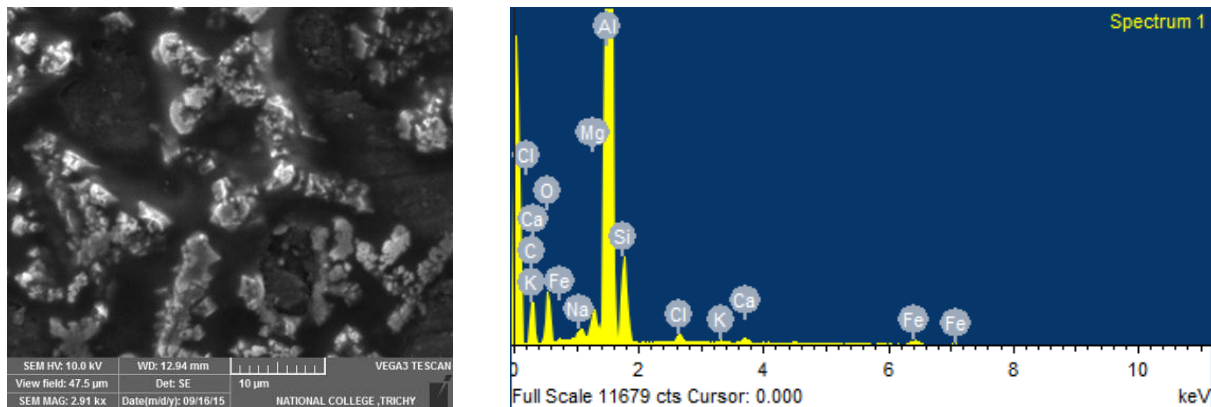


Fig. 21 SEM image of A356 -8% vol MWCNT

Fig. 22 EDAX image of A356 composite reinforced with 8% vol MWCNT

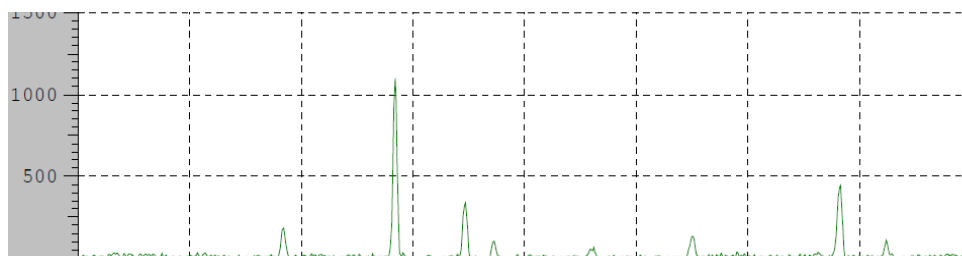


Fig. 23 XRD spectrum of A356 composite reinforced with 8% vol MWCNT

The microhardness of pure A356 alloy, its composites and gray cast iron are determined using microhardness testing machine using vickers scale. In a sample readings are taken in ten different locations with a pitch distance of one millimeter. The average value of microhardness obtained from all ten locations is taken as the final microhardness value of the material. To observe the relation between micro hardness and reinforcement ratio the hardness values thus obtained are plotted in a bar chart as shown Fig. 24. It is evident from the figure that microhardness increases as the reinforcement ratio increases. The highest microhardness value is recorded with 8% vol MWCNT composite which is greater than the microhardness value of conventional brake drum material (gray cast iron). Because of this highest microhardness possessed by 8% vol composite it exhibits lower wear rate and lesser coefficient friction which are all the favorable characteristics of a good brake drum material.

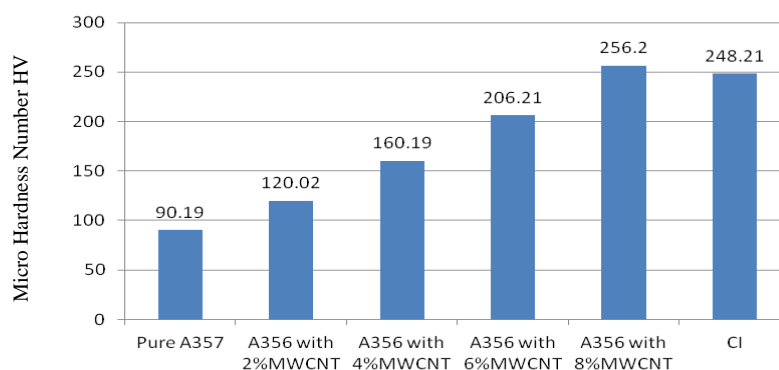


Fig. 24 Micro hardness for samples

IV. EXPERIMENTAL RESULTS

Dry sliding wear tests of the A356 alloy, its composites and gray cast iron against car brake pad material were

conducted at room temperature as per ASTM G99-04 standard in a pin on disc apparatus (DUCOM-make). The cast iron disc was machined from a commercial passenger car brake rotor. The outer diameter and the thickness of all discs are 165mm and 8mm respectively. The surface is machined to an average roughness value of $1.5\mu\text{m}$ which is same as the roughness value of the sliding surface of the actual commercial brake rotor. Fig. 25 shows the photographs of finished discs of A356, MMC and gray cast iron.

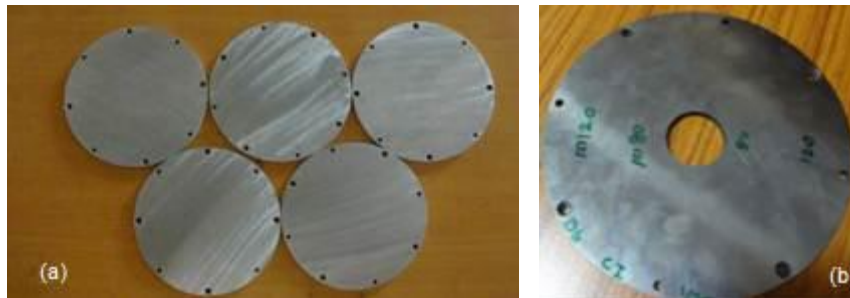


Fig. 25 Machined discs: (a) of A356-MWCNT composite, (b) of gray cast iron

Hardened A356 and its composites' are used as disc material. The size of the pin is $10\text{mm} \times 10\text{mm} \times 35\text{mm}$. Pins are machined from passenger car brake pads as shown in Fig. 26.



Fig. 26 Pins prepared from Car Brake pad Material

A digital balance with an accuracy of 1mg was used to measure the weight of the pin and the discs. Weight-loss measurements technique was used to calculate the wear rate. Friction coefficient is calculated from the frictional force (which was recorded during experiment) and normal applied load using the relation $F = \mu N$. Where N , F and μ represents applied normal load in Newton, frictional force in Newton and coefficient of friction respectively. Data acquisition during the experiment was done using WINDUCOM2010 software with LVDT and load cell as displacement (height reduction of the pin) and force (friction force) sensors respectively. The photographic image of experimental set-up is shown in Fig. 27a. Whereas, Fig. 27 b shows the contact between pin and disc during the experiment.



Fig. 27 DUCOM pin on disc apparatus: (a) experimental set-up, (b) contact between pin and disc

A total of six discs are tested under various sliding and loading conditions. The numbering of discs are as shown in the Table 4. The detailed levels of wear testing parameters are shown in Table 5. Wear rate and co-efficient of friction are evaluated for the discs D1 to D6 by using these levels of parameter. The influence of the normal load, sliding speed and reinforcement ratios on wear and coefficient friction were studied by keeping sliding distance as constant (3000m).

TABLE 4 DETAILS OF DISC SPECIMENS

Disc Number	Material
D1	Pure A356 Aluminum alloy
D2	A356 Aluminum alloy with 2%vol MWCNT
D3	A356 Aluminum alloy with 4%vol MWCNT
D4	A356 Aluminum alloy with 6%vol MWCNT
D5	A356 Aluminum alloy with 8%vol MWCNT
D6	Gray cast iron

TABLE 5 PARAMETERS AND LEVELS OF WEAR TEST

Sliding Velocity (m/s)		Normal Load (N)				Sliding Distance (m)	Discs
		19.62	39.24	58.86	78.48		
	3	✓	✓	✓	✓	3000	D1, D2, D3, D4, D5 and D6
	4	✓	✓	✓	✓		
	5	✓	✓	✓	✓		
	6	✓	✓	✓	✓		

It is observed from Table 5 that a single disc will be subjected to $4 \times 4 = 16$ readings. “✓” mark represents a reading is taken for that sliding velocity and the loading condition. All discs put together will give a total of 96 readings. The photographic view of the sample after wear test is shown in Fig. 28.



Fig. 28 Photographic view of the sample after wear test: (a) D1, D2, D3, D4 and D6 (b) D5

V. ANALYSIS OF RESULTS

A. Wear Rate

Wear rate is defined as the volume loss of the material per unit sliding distance. The effect of applied load (in N) on wear rate (in mm^3/m) and reinforcement ratio (in %) at various sliding velocity are displayed in the Figs. 29-32. All four graphs are showing a common phenomenon that as applied load increases wear rate also increases for all materials (pure A356, its composites, and gray cast iron). Generally at higher loads heat generation will be more due to higher frictional force (frictional force is directly proportional to applied load) as a result of more heat comparatively the material will get soften and leads to a higher wear rate. Then it is further observed from all four graphs that the pure A356 curve is above all curves of composites and gray cast iron. It indicates that irrespective of the sliding velocity pure A356 is subjected to more wear rate under all loading conditions. If we observe further that curves with higher reinforcement ratio are falling below the curves of lower reinforcement ratio. The bottom most curve is having highest reinforcement ratio of 8%vol MWCNT. This trend gives strong evidence that wear rate decreases with increase in reinforcement ratio. It is understood that differences in the coefficient of thermal expansion between the reinforcement particles and matrix leads to the formation of strain field at the interface. As reinforcement ratio increases formation of strain field at the interface of the matrix and reinforcements also increases. As the strain field formation increases hardness of the composites increases leading to lower wear rate of the material. This is the reason that the curves belong to higher reinforcement ratios are falling below the wear curve of pure A356. Particularly the curve belongs to 8%MWCNT is below the gray cast iron curve. This is also another evidence that wear rate of 8%MWCNT is lower than even gray cast iron the conventional material for brake drum.

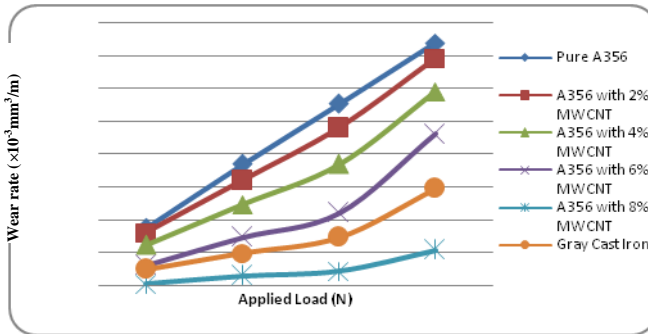


Fig. 29 Load vs. wear rate at 3m/s

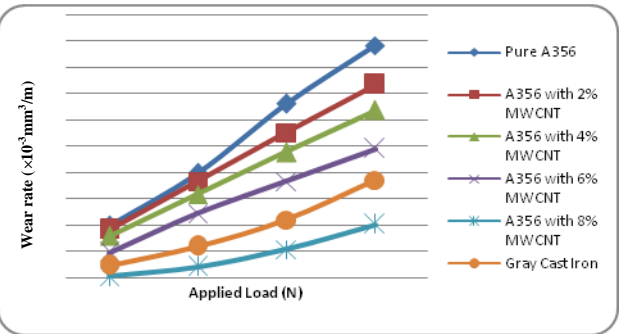


Fig. 30 Load vs. wear rate at 4m/s

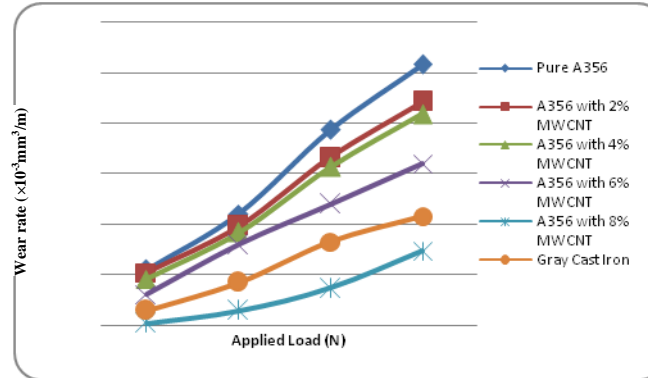


Fig. 31 Load vs. wear rate at 5m/s

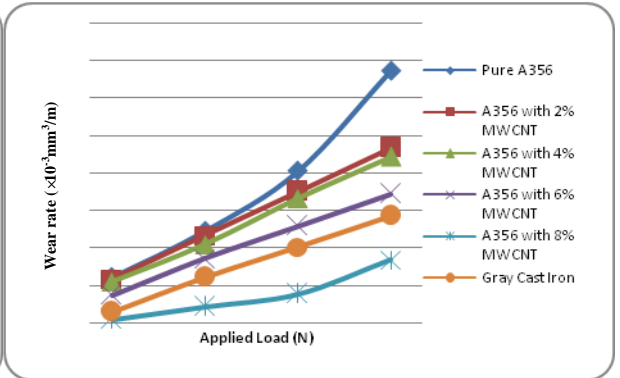


Fig. 32 Load vs. wear rate at 6m/s

The variation of wear rate with change in sliding velocity is being analyzed in Figs. 33-36. Here also a common trend is observed in all the four graphs that as sliding velocity increases wear rate also increase irrespective of the reinforcement ratio. Even though the normal load is kept constant, increase in sliding velocity leads to more kinetic energy, as energy needs to be dissipated due to friction is high that leads to more heat energy which results in relative softening of the material and ultimately give more wear of the material. Because of this higher wear rate is recorded at higher sliding velocities.

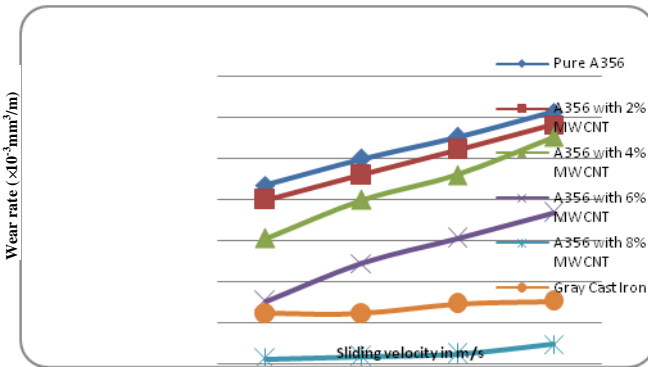


Fig. 33 Sliding velocity vs. wear rate at a load of 19.6N

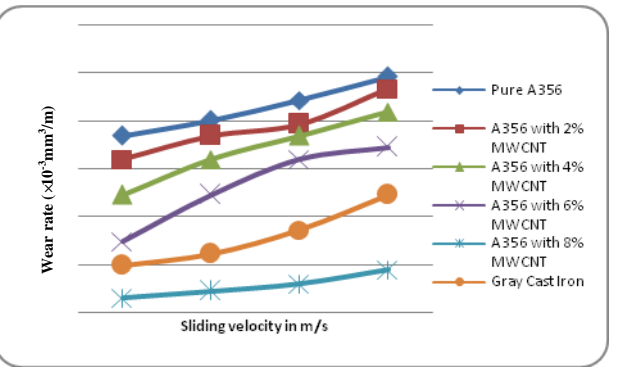


Fig. 34 Sliding velocity vs. wear rate at a load of 39.24

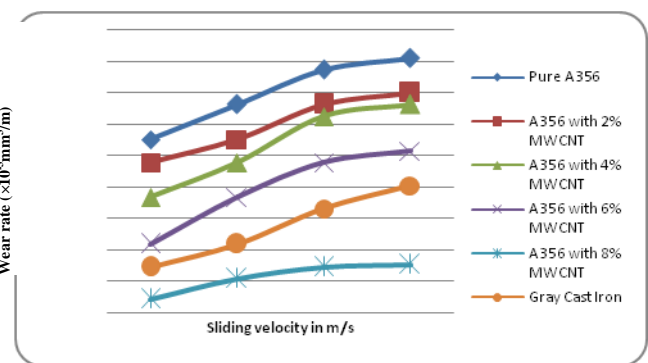


Fig. 35 Sliding velocity vs. wear rate at a load of 58.86N

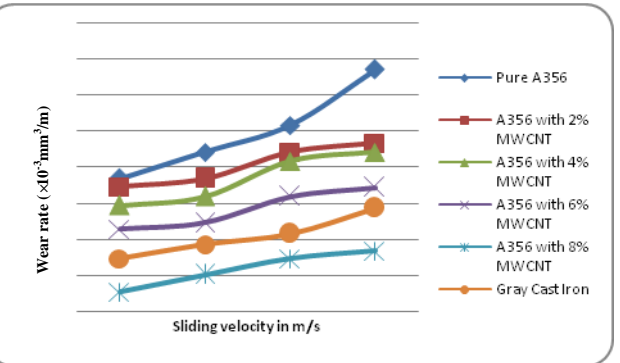


Fig. 36 Sliding velocity vs. wear rate at a load of 78.48N

Another common trend observed from all four figures is that the curves belong to higher reinforcement ratios are falling

below curves of lower reinforcement ratio. Notably pure A356 aluminum alloy curve is occurring above all curves indicating that wear rate is higher than its composites and gray cast iron. As the reinforcement ratio increases wear rate decreases which indicates that addition MWCNT improves the wear resistance of the material. Here also when the reinforcement is 8% vol with MWCNT the wear rate is the least than the gray cast iron. The addition of reinforcements creates a strong bond between reinforcements and matrix, which increase the hardness of the composite. The hardness of the composite is inversely proportional to the wear rate. Hardness of composites is further increased by increasing the reinforcement ratio as shown in Fig. 36. Because of higher hardness possessed by A356 8% vol MWCNT composite is having lesser wear rate than other material including gray cast iron for higher velocities as well as higher loading conditions.

B. Coefficient of Friction

The ratio between friction force and normal load is known as coefficient of friction. The relationship between applied load and reinforcement ratio on coefficient of friction or different sliding velocities are shown in Figs. 37-40. All curves are showing similar trend that coefficient friction increases with applied load. Archard et al. [27] have explained that increase in normal load increases the applied pressure. Therefore, the friction between the pin and counter face increases by increasing the applied pressure. This effect increases the friction coefficient.

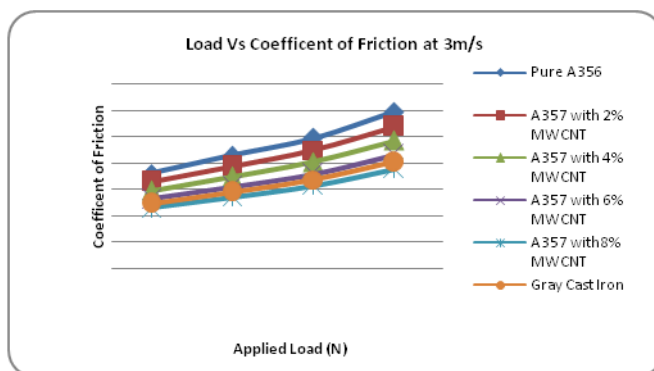


Fig. 37 Load vs. coefficient of friction at 3m/s

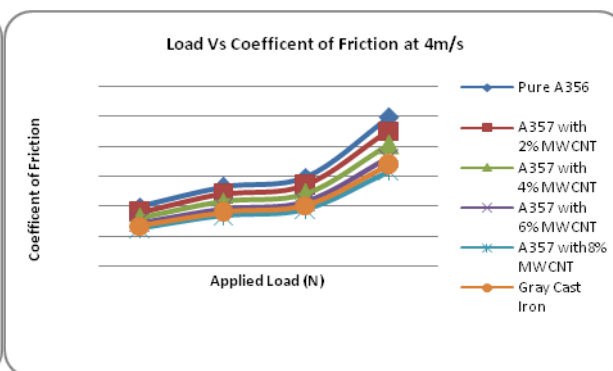


Fig. 38 Load vs. coefficient of friction at 4m/s

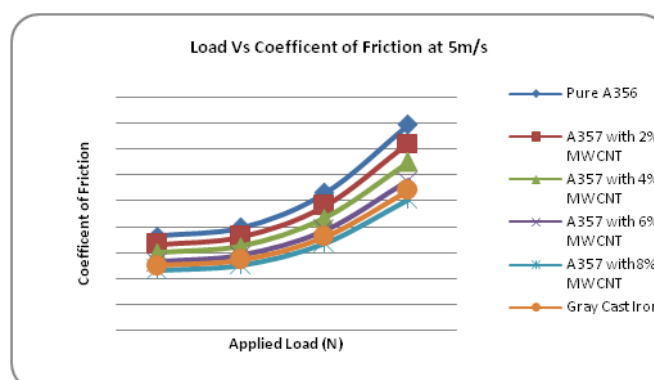


Fig. 39 Load vs. coefficient of friction at 5m/s

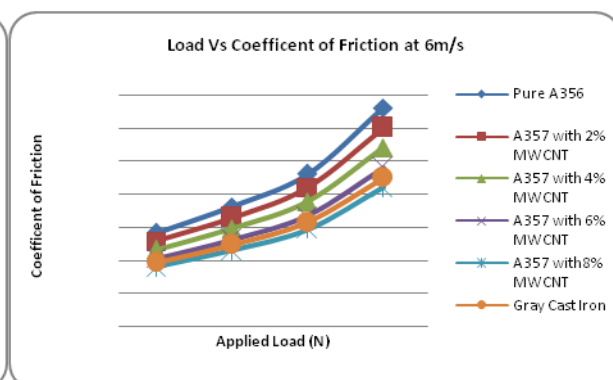


Fig. 40 Load vs. coefficient of friction at 6m/s

Higher coefficient of friction is experienced by unreinforced alloy for all loading conditions. Because of this higher friction coefficient the unreinforced alloy has suffered with higher wear rate than reinforced materials. Unreinforced alloy undergoes plastic deformation due to friction and heat generation at the sliding surface. This deformed surface had induced higher frictional resistance at the sliding surface and increases the friction coefficient. On the other hand addition of reinforcement offers resistance to plastic deformation. Friction coefficients have increased with the decreasing of the content of carbon nanotubes. The nanotubes tend to form a continuous lubricating film of carbon, keeping the upper and lower test pieces from abrading each other and thus the friction coefficient decreased. Therefore, the coefficient of friction is lesser when compared to unreinforced alloy under all loading and sliding conditions. Hence, coefficient of friction decreases by increasing the reinforcement ratio. The effect of sliding speed on coefficient of friction is shown in Figs. 41-44. It is observed from Figures that the coefficient of friction increases by increasing the sliding velocity. Tangential force is minimal when sliding velocity is low. The strain rate and deformation rate on the subsurface is increased at higher velocity, results in increase of friction coefficient.

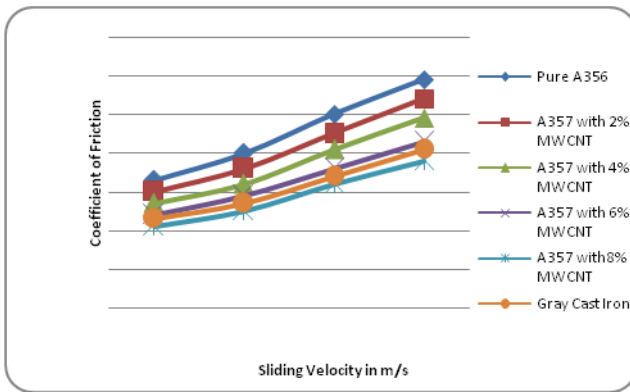


Fig. 41 Sliding velocity vs. coefficient of friction at a load of 19.62N

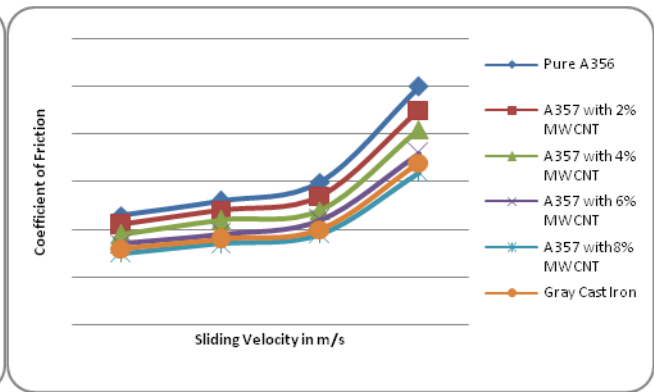


Fig. 42 Sliding velocity vs. coefficient of friction at a load of 39.24N

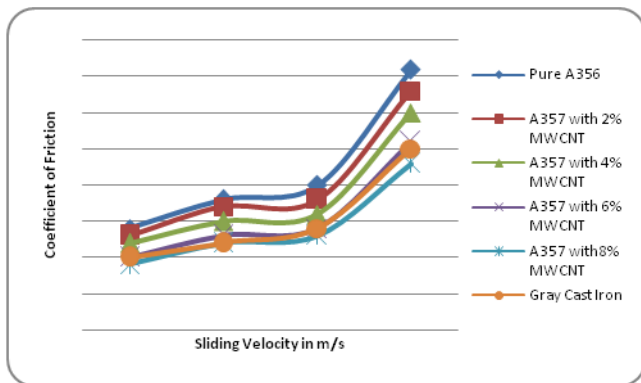


Fig. 43 Sliding velocity vs coefficient of friction at a load of 58.86N

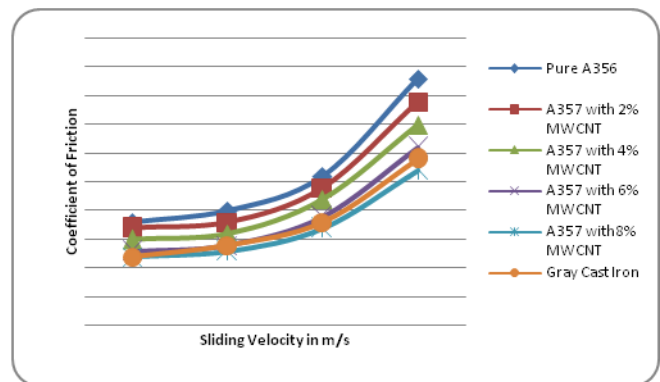


Fig. 44 Sliding velocity vs coefficient of friction at a load of 78.48N

Coefficient of friction evaluated as a function of reinforcement ratio is shown in Figs. 41-44 for different sliding velocities. It is evident from figures that the coefficient of friction for the A356 alloy is more than composites. Wear volume is inversely proportional to the volume fraction of the composites. Thus, increase in the reinforcement ratio reduces loss of wear, which minimizes the friction.

VI. ANALYSIS OF WORN-OUT SURFACES

Samples from worn-out surfaces of six discs specimens used for the study are subjected to SEM analysis. Figs. 45-50 depict the worn surfaces of A356 alloy, A356 composites reinforced with 2%, 4%, 6% and 8% vol. of MWCNT and gray cast iron at 78.48N load, 6m/s sliding velocity and 3000m sliding distance with similar magnification.

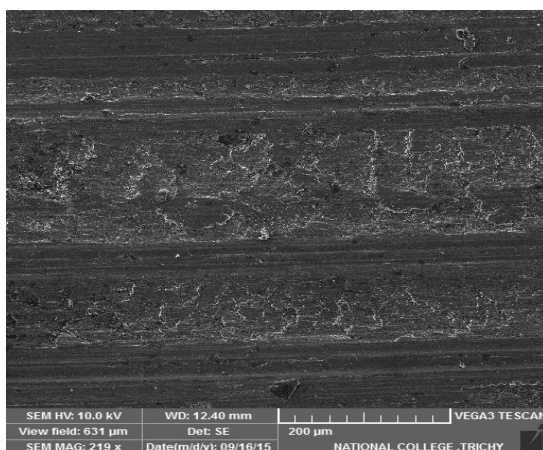


Fig. 45 Worn-out surface of pure A356 alloy

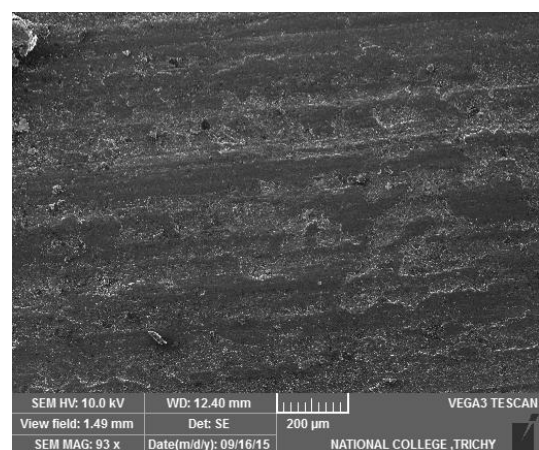


Fig. 46 Worn-out surface of A356 composite with 2%MWCNT

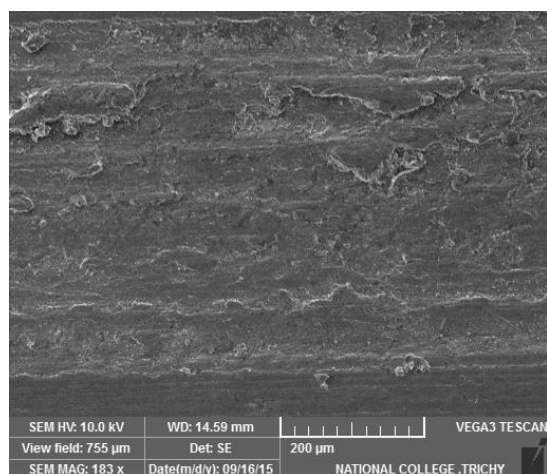


Fig. 47 Worn-out surface of A356 composite with 4%MWCNT

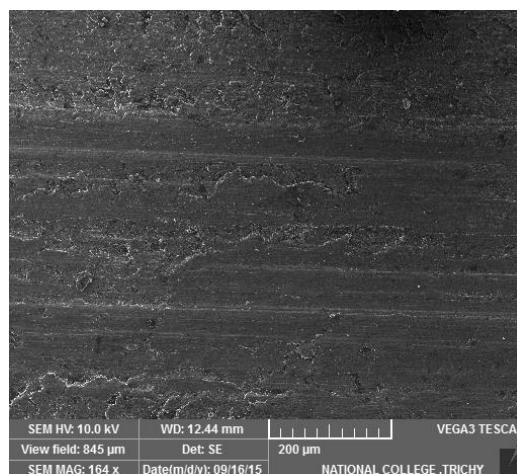


Fig. 48 Worn-out surface of A356 composite with 6%MWCNT

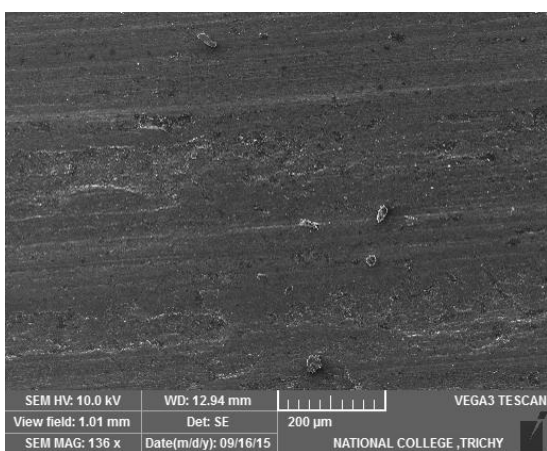


Fig. 49 Worn-out surface of A356 composite with 8%MWCNT



Fig. 50 Worn-out surface of gray cast iron

It is observed that the width of groove along sliding direction is more in Fig. 45 when compared to Fig. 49. The presence of MWCNT reinforcement in composites allows less deformation, whereas more deformation at edge of groove is observed in Fig. 45. The iron-rich debris layer formation on sliding surface is observed in Fig. 49. The composite wear surface (Fig. 49) shows less broken debris, voids, pits, scratches and grooves than the wear surface of the A356 alloy (Fig. 45). The composite with 8% reinforced ratio has lower wear rate than unreinforced A356 alloy. The existence of reinforcement particles in the matrix offers resistance to initiate cracks. The longitudinal load through sliding disc initiates the voids around the particle. These particles are removed under further loading. Fine and uniformly distributed reinforcements protect the soft matrix from erosion during sliding. Niranjana et al. [33] categorized the wear mechanism under different loading conditions namely mild wear, severe wear and ultra-fine wear. From this observation, the wear mechanism in Fig. 49 is mild wear with abrasive wear mechanism. Figure 45 indicates high degree of deformation due to load of 78.48N, when compared other Fig. 46 to 47 and 50 for similar conditions. It is observed from figures that there is more quantity of broken debris layer, broken reinforcement particles, voids and deep grooves. High temperature and thermal softening at the sliding surface facilitates to remove reinforcement particles from matrix easily. Koji and Koshi [22] categorized the nature of contact between pin and disc into mechanical severity contact and thermal severity contact. The above observation belongs to thermal severity contact category. Therefore, the wear mechanism of unreinforced composite under 78.48N load, 6m/s sliding speed and sliding distance of 3000m is follows delaminate wear.

VII. CONCLUSION

Wear test for the A356 alloy, its composites and gray cast iron are conducted at room temperature under dry sliding conditions. The following conclusions are drawn from the results, discussions and observations from worn surfaces:

- Wear rate and coefficient of friction are influenced by normal load, reinforcement ratio and sliding speed.
- Wear and friction properties of A356 alloy was improved with addition of MWCNT reinforcements.
- Both wear rate and coefficient of friction were increased with the increase of normal load and vice versa.
- Both wear rate and coefficient of friction were increased with the increase of sliding speed and vice versa.
- Both wear rate and coefficient of friction decreases by increasing the reinforcement ratio.

- Worn-out surface analysis indicates that the debris layer formation on the sliding surfaces plays a significant role in wear and friction characteristics.
- The wear mechanism is characterized as mild wear at lower reinforcement ratio, severe wear at moderate reinforcement ratio, and ultra-fine wear at higher reinforcement ratio.
- The A356 8% vol. MWCNT is having superior performance of low wear rate and low coefficient of friction as compared with all other composites, unreinforced alloy and gray cast iron.
- In conclusion A356 8% vol. MWCNT can be a better replacement for conventional brake drum material such as gray cast iron which could result in 60% weight reduction of brake drum. This will help the automobile to improve the fuel economy.

ACKNOWLEDGMENT

The authors acknowledge and express deep gratitude to Kalinga University, Raipur, India; Karunya University, Coimbatore, India; and National College, Trichy, India for extending their support and providing research facilities to carry out this research work.

REFERENCES

- [1] R. Shadakshari, K. Mahesha, and H. B. Niranjana, "Carbon nanotube reinforced aluminium matrix composites – a review," *International Journal of Innovative Research in Science, Engineering and Technology*, vol. 1, iss. 2, pp. 74-80, December 2012.
- [2] T. Thirerujirapong, K. Kondoh, J. Umeda, and H. Imai, "Friction and wear behavior of titanium matrix composite reinforced with carbon nano tubes under dry conditions," *Transactions of JWRI*, vol. 37, no. 2, pp. 51-56, 2008.
- [3] N. Al-Aqeeli, "Processing of CNTs reinforced Al-based nanocomposites using different consolidation techniques," *Journal of Nanomaterials*, Article ID 370785, 10 pages, 2013.
- [4] Z.Y. Liu, B.L. Xiao, W.G. Wang, and Z.Y. Ma, "Singly dispersed carbon nanotube/aluminum composites fabricated by powder metallurgy combined with friction stir processing," *Carbon*, vol. 50, pp. 1843-1852, 2012.
- [5] Jinzhi Liao, Ming-Jen Tan, Raju V. Ramanujan, and Shashwat Shukla, "Carbon nanotube evolution in aluminum matrix during composite fabrication process," *Materials Science Forum*, vol. 690, pp. 294-297, 2011.
- [6] S. Ko, B. Kim, Y. Kim, T. Kim, K. Kim, B. McKay, and J. Shin, "Manufacture of CNTs-Al powder precursors for casting of CNTs-Al matrix composites," *Materials Science Forum*, vol. 765, pp. 353-357, 2013.
- [7] J. D. Kim, J. H. Park, J. H. Cha, and S. I. Jung, "Control of mechanical properties according to content ratio of copper coated carbon nanotubes in aluminum composites," *18th International Conference on Composite Materials*, S. Korea, 2011. Available from: [http://www.iccm-central.org/Proceedings/ICCM18proceedings/data/3.%20Poster%20Presentation/Aug24\(Wednesday\)/P3-16~63%20Nanocomposites/P3-35-IK0462.pdf](http://www.iccm-central.org/Proceedings/ICCM18proceedings/data/3.%20Poster%20Presentation/Aug24(Wednesday)/P3-16~63%20Nanocomposites/P3-35-IK0462.pdf).
- [8] H. Kwon and M. Leparoux, "Fabrication of functionally graded carbon nanotube-reinforced aluminum matrix composite," *Advanced Engineering Materials*, vol. 13, no. 4, pp. 325-329, April 2011.
- [9] R. Unnikrishnan, M. S. Renjith, J. Aneesh Kumar, and T. Krishnakumar, "Processing and characterization of aluminium-silver coated MWCNT composite made by vacuum hot pressing," *International Journal of Modern Engineering Research*, vol. 2, iss. 3, pp. 1167-1170, May-June 2012.
- [10] Kwon H and Kim S., et al., "Carbon nanotube gradient layers reinforced aluminum matrix composite materials," *18th International Conference on Composite Materials*, S. Korea, 2011. Available from: [http://www.iccm-central.org/Proceedings/ICCM18proceedings/data/3.%20Poster%20Presentation/Aug24\(Wednesday\)/P3-1~15%20Multi-functional%20Composites/P3-2-IK1577.pdf](http://www.iccm-central.org/Proceedings/ICCM18proceedings/data/3.%20Poster%20Presentation/Aug24(Wednesday)/P3-1~15%20Multi-functional%20Composites/P3-2-IK1577.pdf).
- [11] N. A. Baena, W. Salas, and L.E. Murr, *Shock-wave-compaction (SWC) of Al/CNT two phase systems*, Carbon Nanotubes, Jose Mauricio Marulanda, Ed., ISBN: 978-953-307-054-4, InTech, 2010. Available from: <http://www.intechopen.com/books/carbon-nanotubes/shock-wave-compaction-swc-of-al-cnttwo-phase-systems.com>.
- [12] D.K. Lima, T. Shibayanagib, and A.P. Gerlich, "Synthesis of multi-walled CNT reinforced aluminum alloy composite via friction stir processing," *Materials Science and Engineering A*, vol. 507, pp. 194-199, 2009.
- [13] B. Abbasipour, B. Niroumandn, and S. M. MonirVaghefi, "Compocasting of A356-CNT composite," *Trans. Nonferrous Met. Soc. China*, vol. 20, pp. 1561-1566, 2010.
- [14] T. Laha, A. Agarwal, Tim McKechnie, and S. Seal, "Synthesis and characterization of plasma spray formed carbon nano tube reinforced aluminum composite," *Materials Science and Engineering A*, vol. 381, pp. 249-258, 2004.
- [15] T. Noguchi, A. Magario, S. Fukazawa, S. Shimizu, J. Beppu, and M. Seki, "Carbon nanotube/aluminium composites with uniform dispersion," *Materials Transactions*, vol. 45, no. 2, pp. 602-604, 2004.
- [16] M.S. Senthil Saravanan, S.P. Kumaresw Babu, and K. Sivaprasad, "Mechanically Alloyed Carbon Nanotubes (CNT) Reinforced Nanocrystalline AA 4032: Synthesis and Characterization," *Journal of Minerals & Materials Characterization & Engineering*, vol. 9, no. 11, pp. 1027-1035, 2010.
- [17] Y. Morisada, H. Fujii, T. Nagaoka, and M. Fukusumi, "MWCNTs/AZ31 surface composites fabricated by friction stir processing," *Materials Science and Engineering A*, vol. 419, pp. 344-348, 2006.
- [18] D. Lu, Y. Jiang, and R. Zhou, "Wear performance of nano-Al₂O₃ particles and CNTs reinforced magnesium matrix composites by friction stir processing," *Wear*, vol. 305, pp. 286-290, 2013.

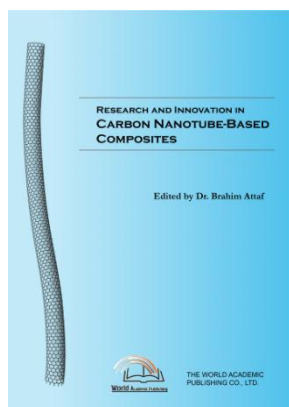
- [19] C.B. Lin, Zue-Chin Changb, Y.H. Tunga, and Y.Y. Ko, "Manufacturing and tribological properties of copper matrix/carbon nano-tubes composites," *Wear*, vol. 270, pp. 382-394, 2011.
- [20] M. K. Habibi, A.M.S. Hamouda, and M. Gupta, "Enhancing tensile and compressive strength of magnesium using ball milled Al+CNT reinforcement," *Composites Science and Technology*, vol. 72, pp. 290-298, 2012.
- [21] O. Carvalho, M. Buciumeanu, S. Madeira, D. Soares, F.S. Silva, and G. Miranda, "Optimization of AlSi-CNTs functionally graded material composites for engine piston rings," *Materials and Design*, vol. 80, pp. 163-173, 2015.
- [22] K. Koji and A. Koshi, "Wear of advanced ceramics," *Wear*, vol. 253(11-12), pp. 1097-104, 2002.
- [23] N. Silvestre, B. Faria, and J.N. C Lopes, "Compressive behavior of CNT-reinforced aluminum composites using molecular dynamics," *Composites Science and Technology*, vol. 90, pp. 16-24, 2014.
- [24] T. Peng and I. Chang, "Mechanical alloying of multi-walled carbon nanotubes reinforced aluminum composite powder," *Powder Technology*, vol. 266, pp. 7-15, 2014.
- [25] A.M.K. Esawi, K. Morsi, A. Sayed, M. Taher, and S. Lanka, "The influence of carbon nanotube (CNT) morphology and diameter on the processing and properties of CNT-reinforced aluminium composites," *Composites: Part A*, vol. 42, pp. 234-243, 2011.
- [26] J. Liao and M.J. Tan, "Mixing of carbon nanotubes (CNTs) and aluminum powder for powder metallurgy use," *Powder Technology*, vol. 208, pp. 42-48, 2011.
- [27] I. Alfonso, O. Navarro, J. Vargas, A. Beltrán, C. Aguilar, G. González, and I. A. Figueroa, "FEA evaluation of the Al₄C₃ formation effect on the Young's modulus of carbon nanotube reinforced aluminum matrix composites," *Composite Structures*, vol. 127, pp. 420-425, 2015.
- [28] B. Chen, S. Li, H. Imai, L. Jia, J. Umeda, M. Takahashi, and K. Kondoh, "An approach for homogeneous carbon nanotube dispersion in Al matrix composites," *Materials and Design*, vol. 72, pp. 1-8, 2015.
- [29] S. Zhou, X. Zhang, Z. Ding, C. Min, G. Xu, and W. Zhu, "Fabrication and tribological properties of carbon nanotubes reinforced Al composites prepared by pressureless infiltration technique," *Composites: Part A*, vol. 38, pp. 301-306, 2007.
- [30] X. Yang, C. Shi, C. He, E. Liu, J. Li, and N. Zhao, "Synthesis of uniformly dispersed carbon nanotube reinforcement in Al powder for preparing reinforced Al composites," *Composites: Part A*, vol. 42, pp. 1833-1839, 2011.
- [31] A. Esawi and K. Morsi, "Dispersion of carbon nanotubes (CNTs) in aluminum powder," *Composites: Part A*, vol. 38, pp. 646-650, 2007.
- [32] H. J. Choi, B. H. Min, J. H. Shin, and D. H. Bae, "Strengthening in nanostructured 2024 aluminum alloy and its composites containing carbon nanotubes," *Composites: Part A*, vol. 42, pp. 1438-1444, 2011.
- [33] K. Niranjana and P. R. Lakshminarayanan, "Dry sliding wear behaviour of in-situ Al-TiB₂ composites," *Materials and Design*, vol. 47, pp. 167-73, 2013.



Meenakshi Sundaram. U was born in Kallorani a small village in Tamil Nadu state, India on 9th July 1977. He is holding Bachelor of Engineering degree in Mechanical Engineering from Manonmanium Sundaranar University, Tirunelveli, Tamilnadu, India; Master of Technology in Mechanical Design from IASE University, Sardharshar, Rajasthan, India, and Master of Technology in Human Resource Development from University of Madras, Chennai, Tamil Nadu, India. He is pursuing his PhD in Mechanical Engineering in the research area of nano composite materials with Kalinga University, Raipur, Chattisgarh, India. He is having 14 years of teaching experience in Engineering College and Universities both in India and in abroad. Currently he is working as Lecturer in The Department of Mechanical Engineering, Dilla University, Ethiopia. He has authored course materials on Engineering Design, Mechanical Vibrations and Mechanics of Machines. His Research interest includes Nano-composite materials, Human Centered Design and Macro-ergonomics. **Mr. Meenakshi** is a life member of Indian Society for Technical Education, New Delhi India and Associate Member of Institution Engineers (India), Kolkatta.



Professor A. Mahamani works in the Department of Mechanical Engineering, Sri Venkateswara College of Engineering and Technology, Chittoor. He obtained his PhD in Mechanical Engineering from Jawaharlal Nehru Technological University, Anantapur. He also obtained his Master's Degree in Production Engineering from Annamalai University, Chidambaram and Bachelor's Degree in Mechanical Engineering from Madras University. He published 25 papers in International Journals, 13 papers in National Level Journals and 27 papers in conference proceedings. Dr. Mahamani received Rs 38 Lakhs through grants for research promotion, Laboratory modernization and organizing seminars. He had chaired, organized, and conducted numerous workshops, seminars and conferences. Dr. Mahamani received a couple of best paper award in IEEE sponsored International conference. His biographical note appeared in the International Biographical Centre, Cambridge, England as one of the Top 100 professionals 2013 and Reference Asia: Asia's Who's who of men of achievement-2013. He received fast track young scientist research grant from Department of Science and Technology and Research award from University Grant commission India.



Research and Innovation in Carbon Nanotube-Based Composites
Edited by Dr. Brahim Attaf

ISBN 978-0-9889190-1-3

Hard cover, 136 pages

Publisher: The World Academic Publishing Co. Ltd.

Published in printed edition: 30, December 2015

Published online: 30, December 2015

This book of nanoscience and nanotechnology provides an overview for researchers, academicians and industrials to learn about scientific and technical advances that will shape the future evolution of composite materials reinforced with carbon nanotubes (CNTs). It involves innovation, addresses new solutions and deals with the integration of CNTs in a variety of high performance applications ranging from engineering and chemistry to medicine and biology. The presented chapters will offer readers an open access to global studies of research and innovation, technology transfer and dissemination of results and will respond effectively to challenges related to this complex and constantly growing subject area.

How to cite this book chapter

Meenakshi Sundaram. U and Mahamani. A (2015). Development of Carbon Nanotube Reinforced Aluminum Matrix Composite Brake Drum for Automotive Applications, *Research and Innovation in Carbon Nanotube-Based Composites*, Dr. Brahim Attaf (Ed.), ISBN 978-0-9889190-1-3, WAP-AMSA, Available from: <http://www.academicpub.org/amsa/>

World Academic Publishing - Advances in Materials Science and Applications

